Biophysical Chemistry 147 (2010) 104–110

Contents lists available at ScienceDirect

Biophysical Chemistry

journal homepage: http://www.elsevier.com/locate/biophyschem

Characterization of condensed plasmid DNA models for studying the direct effect of ionizing radiation

Mandi Tsoi [a], Trinh T. Do [a], Vicky Tang [a], Joseph A. Aguilera [a], Christopher C. Perry [b], Jamie R. Milligan [a,*]

[a] Department of Radiology, University of California at San Diego, 9500 Gilman Drive, La Jolla, CA 92093-0610, United States
[b] Department of Biochemistry, Mortensen Hall, Loma Linda University, 11085 Campus Street, Loma Linda, CA 92350, United States

ARTICLE INFO

Article history:
Received 24 November 2009
Received in revised form 19 December 2009
Accepted 19 December 2009
Available online 4 January 2010

Keywords:
DNA condensation
DNA damage
Gamma irradiation
Ligand
Atomic force microscopy
Circular dichroism

ABSTRACT

We have examined the changes in physical properties of aqueous solutions of the plasmid pUC18 that take place on the addition of the cationic oligopeptide penta-arginine. An increase in sedimentation rate and static light scattering, and changes in the nucleic acid CD spectrum all suggest that this ligand acts to condense the plasmid. Dynamic light scattering suggests the hydrodynamic radii of the condensate particles are a few micrometers, *ca.* 50-fold larger than that of the monomeric plasmid. Condensation of the plasmid also produces a *ca.* 100-fold decrease in the strand break yield produced by gamma irradiation. This extensive protection against reactive intermediates in the bulk of the solution implies that condensed plasmid DNA may offer a model system with which to study the direct effect of ionizing radiation (ionization of the DNA itself). The use of peptide ligands as condensing agents in this application is attractive because the derivatives of several amino acids (particularly tryptophan and tyrosine) have been shown to modify the radiation chemistry of DNA extensively.

1. Introduction

DNA condensation has been studied for many years for two principal reasons [1]. The first motivation is to study the energetics of the compact arrangement of DNA in naturally occurring structures such as phage and viral particles and chromosomes. Another is the development of non-viral genetic therapy delivery vehicles. Lengthy DNA molecules in phage and virus particles, and especially in the nuclei of cells, are naturally highly compacted into small volumes. DNA compaction also facilitates its penetration of the membrane from outside of the cell and is central to the development of methods for gene transfer that seeks to avoid viral transduction.

The mechanism of condensation may involve both compaction, where the volume occupied by a single DNA molecule is substantially decreased, and also aggregation in which multiple DNA molecules are bound together. Agents capable of condensing DNA include the substitution inert complex ion hexa-ammine cobalt (III) [2], polyamines such as spermidine and spermine [3], cationic (also described as basic) proteins [4,5], artificial polymers [6], and cosolvents [7]. In several cases a distinctive toroidal morphology has been reported for DNA condensates [8,9], although spherical and elongated structures have also been observed [10].

The condensed form of DNA is able to approximate the very highly compact conformations found in phage and viral capsules, where the DNA concentration is as high as *ca.* 800 mg mL^{-1} [11]. Moreover, the condensed DNA model system is a good approximation for the chromatin of mammalian cells where the DNA concentration in a metaphase chromosome is *ca.* 170 mg mL^{-1} [11]. From the point of view of radiation chemistry and radiation biology, the properties of condensed DNA make it a valuable tool for improving our understanding of the relative contributions made to DNA damage by the direct, quasi-direct, and indirect effects of ionizing radiation [12].

The direct effect is the mechanism by which chemical modification of the DNA results from ionization of the DNA itself. In the indirect effect, ionization of the solvent produces highly reactive intermediates. These intermediates, or species derived from them by reactions with solutes, may chemically modify the DNA by reacting with it. These two mechanisms can be distinguished because DNA damage resulting from the indirect effect can be attenuated by competing for the reactive intermediates with scavengers. The quasi-direct effect refers to solvent ionization so close to the DNA that subsequent charge transfer to the DNA is faster than the release of diffusible intermediates [13]. It makes an important contribution only for the most closely associated hydration layer of about 10 water molecules per nucleotide residue [14]. In contrast the metaphase chromosome DNA concentration of 170 mg mL^{-1} [11] corresponds to a hydration level of 90 to 100 H_2O per nucleotide residue. Using living cells in the presence of high concentrations of non-toxic cryo-protecting scavengers such as glycerol and DMSO suggests that the indirect effect contributes about 70% of the lethal effects of X- or gamma-irradiation [15,16]. The persistence of a residual lethality is ascribed to the direct effects. The contribution of the direct effects is expected to increase for more

* Corresponding author. Tel.: +1 858 534 4919; fax: +1 858 534 0265.
E-mail address: jmilligan@ucsd.edu (J.R. Milligan).

0301-4622/$ – see front matter © 2010 Elsevier B.V. All rights reserved.
doi:10.1016/j.bpc.2009.12.006

densely ionizing forms of radiation, described as high linear energy transfer (LET) with their lower yields of diffusible reactive intermediates [17]. Examples are neutrons, alpha particles, and fission fragments.

DNA targets in dilute aqueous solution provide an effective model system with which to examine the indirect effect, because it is by far the dominant process under such conditions. To a first approximation the fraction of the energy deposited in the DNA (and producing DNA damage via the direct effect) is equal to the fraction of the mass it contributes to the solution [18]. For typical experimental DNA concentrations in the 0.001 to 1 mg mL^{-1} range, this fraction is below 0.1% and is overwhelmed by the indirect effect. The use of such systems has greatly advanced the understanding of the indirect effect [19]. However, to examine the direct effect against such an enormous background is impossible. Model systems for studying the direct effect extensively suppress the indirect effect by using scavengers [20], cryogenic temperatures [21], and/or dehydration [22]. These methods operate by respectively intercepting the reactive intermediates, preventing their diffusion, or preventing their formation. While they represent rational physical approaches to decreasing the contribution of the indirect effect, by the standards of biochemistry the experimental conditions required are extremely severe. Inherent in the use of scavengers in the first method is the assumption that the secondary radical products of the reaction between the scavenger and the reactive intermediates can be ignored. This assumption appears in many cases to be invalid [23,24]. The last two methods also unavoidably attenuate the reactivity of organic radical species with molecular oxygen. This reaction is rapid and expected to be very important in aqueous solutions [19,25]. It is not clear that observations made under such harsh conditions are directly relevant to those made with mammalian cells under physiological conditions and in general our understanding of the direct effect is poor in comparison to that of the indirect effect.

The use of condensed DNA offers the possibility of developing an alternative model system for the direct effect. It is attractive for several reasons. Condensation produces an extensive attenuation of the indirect effect under mild conditions in room temperature aqueous solution [26]. It is easily reversed by minor changes to the composition of the solution, for example the ionic strength [26]. The distance between the axes of adjacent double helices in condensed DNA has been reported as 2 to 3 nm [27] and the superhelical pitch in the nucleosome lies within this range [28]. Although the detailed structures are no doubt very different, the packing density and solvent accessibility are evidently comparable. As discussed above a wide range of condensing agents is available from which to choose, and polyamines have been studied in connection with radiation effects [29–31].

The presence during ionizing irradiation of simple monomeric amide and ester derivatives of the redox active amino acids cysteine, cystine, histidine, methionine, tryprophan, and tyrosine has been shown to modify the radiation chemistry of DNA [32,33]. The mechanism responsible appears to be electron donation from the amino acid to a radical cation site on the guanine bases of the DNA. It appears likely that this mechanism would operate for regions of DNA that are tightly associated with DNA binding proteins. It is known that the tight binding of the DNA by the protein confers protection against damage by the indirect effect (attack by solvent radicals). To develop a model system with which to study in a systematic fashion how the interaction between DNA binding proteins and DNA affects their radiation chemistry, it is necessary to provide protection against the indirect effect and also to place a redox amino acid residue in close proximity to the DNA. It is possible to synthesize a ligand in which an amino acid is covalently linked to a cationic polyamine such as spermine. But it is far simpler to employ a cationic oligopeptide for this purpose since peptide ligands have the advantage that they can easily accommodate the presence of additional amino acids that have been shown in other systems to modify the DNA damage produced by the direct effect [32]. The use of an intact histone protein would provide results that would be difficult to interpret because of the large number of different amino acid residues that are present.

We report here the use of oligoarginine peptides as condensing agents for plasmid DNA, the resulting protection against DNA damage by the indirect effect, the characterization of the resulting condensates with standard physical methods.

2. Materials and methods

2.1. Sources of biochemicals

A sample of plasmid pUC18 was obtained commercially (Invitrogen, Carlsbad, CA). It was grown in transformed bacterial cells on a mg scale, isolated, and purified as described previously [20]. The oligopeptide penta-arginine (R_5^{5+}) was obtained commercially (Biomatik, Wilmington, DE).

2.2. Sedimentation

The fraction of the plasmid remaining in solution after centrifugation at 15,000×g for 10 min at 25 °C was quantified from the absorbance at $\lambda = 260$ nm of the supernatant using a model DU-800 spectrophotometer (Beckman Coulter, Fullerton, CA).

2.3. Static light scattering

SLS measurements were made using a Hitachi model F-7000 fluorescence spectrometer with both excitation and emission monochromators set to $\lambda = 350$ nm (bandwidth 5 nm). The angle between the incident and scattered light paths was 90°. The sample (200 μL) was contained in a quartz cuvette (1 mL total volume).

2.4. Ethidium fluorescence

Fluorescence measurements were also made with a Hitachi model F-7000 instrument. The displacement of ethidium from the plasmid was assayed using the decrease in fluorescence (excitation 510 nm, bandwidth 5 nm; emission 590 nm, bandwidth 10 nm). The fluorescence polarization was also quantified under these conditions. The ethidium was pre-bound to the plasmid before addition of the ligand. The solutions contained sodium phosphate (5×10^{-3} mol L^{-1}), glycerol (1×10^{-4} mol L^{-1}), ethidium bromide (1×10^{-6} mol L^{-1}), pUC18 plasmid DNA (10 μg mL^{-1}), and penta-arginine (zero to 2×10^{-4} mol L^{-1}).

2.5. Dynamic light scattering

DLS measurements were made with a Nicomp model 370 submicron particle sizing system at a He–Ne laser wavelength of $\lambda = 632$ nm and a power output of 60 mW. All data was collected at a temperature of 25 °C at a scattering angle of 90° with a square acrylic cuvette (3 mL volume) containing a suspension of diffusible particles. Individual solutions of the plasmid and of the ligand were passed through 0.45 μm syringe filters prior to mixing. Brownian motion of these particles produces a time dependent variation in the intensity of the scattered light [34]. This is fitted by a proprietary auto-correlation function which makes no a priori assumption about the shape of the final distribution of the diffusion coefficient D. The general mathematical procedure which is utilized in this analysis is a non-linear least-squares inverse Laplace transform. The hydrodynamic radius R is derived from the diffusion coefficient D using $R = kT/6\pi\eta D$. The parameters k, T, and η represent respectively the Boltzmann constant, absolute temperature, and solvent viscosity. Values for water of the refractive index $n = 1.33$, and $\eta = 8.9\times10^{-4}$ Ns m^{-2} were assumed to be applicable to the solution. For the Nicomp 370, for smaller

particle sizes less than 150 nm, the intensity of the scattered light is proportional to the square of the particle volume. For larger sizes the intensity is diminished from this value due to intraparticle interference effects and the intensity is proportional to the cube of the particle volume.

2.6. Circular dichroism

CD spectra were collected with a Jasco model J-715 spectropolarimeter using a 1 mm path-length 0.3 mL quartz cuvette at 25 °C. Spectra were averaged over 12 scans.

2.7. Atomic force microscopy

The images were collected with a Dimension 5000 instrument (Veeco, Santa Barbara, CA) operated in the tapping mode. The cantilevers (Arrow NCR-50, Nanoworld, Neuchatel, Switzerland) were 160 μm long with a resonant frequency of 285 kHz and a force constant of 42 N m^{-1}. The scan speed was 1 line of 256 pixels per second. The images are topographic (intensity corresponds to height). The samples were prepared by depositing a 5 μL aliquot onto a freshly cleaved mica surface (1 cm × 1 cm) followed by air drying. The samples were not deposited in the presence of any additional cations (such as the commonly employed Mg^{2+} [35,36]), nor were they rinsed. Minor image processing was used in some cases to remove horizontal scanning artifacts and to improve contrast.

2.8. Gamma irradiation

Aliquots (18 μL) of plasmid solutions were aerobically irradiated using ^{137}Cs gamma rays (662 keV) in a GammaCell-1000 device (J.L. Shepherd, San Fernando, CA). The dose rate of 288 rad min^{-1} (4.8×10^{-2} Gy s^{-1}) was quantified with the Fricke system [18] and lithium fluoride thermoluminescence (Landauer, Glenwood, IL).

2.9. Agarose gel electrophoresis

After irradiation the yield of DNA single stand breaks (SSB) was quantified by using agarose gel electrophoresis to separate the supercoiled and open circle forms of the plasmid. Condensation of the plasmid sample (18 μL) was reversed by addition of a conventional loading buffer (4 μL) additionally containing sodium perchlorate to a final concentration of 0.12 mol L^{-1}. The procedures for digital video imaging of ethidium fluorescence and for estimating the *G*-value for SSB formation have been described previously [20].

Briefly, the D_0 radiation dose is that required to decrease the fraction of the SSB free super-coiled form of the plasmid by a factor of *e*. Assuming a Poisson distribution, this decrease corresponds to a mean of one SSB per plasmid, so that concentration of SSB products is equal to the plasmid concentration. Numerically the value of D_0 is equal to the reciprocal of the slope *m* of a straight line fitted to a semi logarithmic yield dose plot. An example is provided in the Results section. Assuming a relative molecular mass of 325 g mol^{-1} per nucleotide residue, a plasmid concentration of 10 μg mL^{-1} is equivalent to 3.1×10^{-5} mol L^{-1} nucleotides. Further assuming the length of pUC18 as 2686 base pairs, this is equivalent to a plasmid concentration of $3.1 \times 10^{-5}/(2 \times 2686) = 5.8 \times 10^{-9}$ mol L^{-1}. The *G*-value for SSB formation is equal to the quotient of this concentration with the D_0 dose.

3. Results

The precipitation assay whose results are plotted in Fig. 1 demonstrates the increased sedimentation rate of the plasmid in the presence of penta-arginine (R_5^{5+}) concentrations greater than about 1×10^{-5} mol L^{-1}. The fraction of the plasmid remaining in solution after centrifugation is undetectably small. This assay has been employed to detect DNA condensation by the cationic peptide penta-lysine [37].

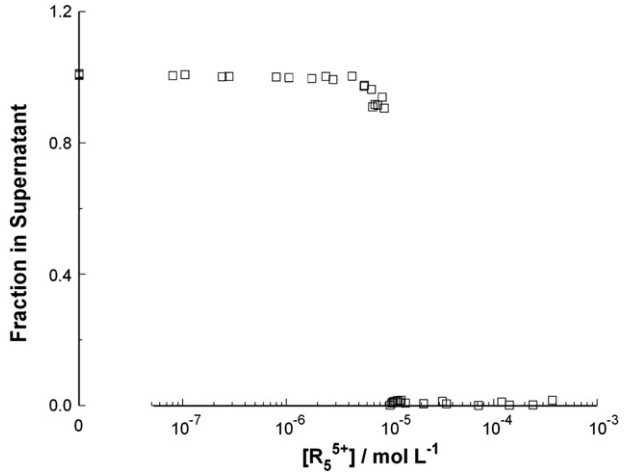

Fig. 1. Effect of penta-arginine (R_5^{5+}) concentration on sedimentation of pUC18 plasmid DNA. The penta-arginine concentration at the *Y*-axis is zero. The solutions contained pUC18 (10 μg mL^{-1}), sodium phosphate (5×10^{-3} mol L^{-1}, pH 7.0), glycerol (1×10^{-4} mol L^{-1}), and penta-arginine (zero to 1×10^{-4} mol L^{-1}). After centrifugation, the pUC18 concentration in the supernatant fraction was quantified by its UV absorbance.

An example of typical light scattering behavior is shown in Fig. 2. Here the intensity of the 350 nm light scattered at 90° is plotted as a function of the concentration of the ligand penta-arginine. A sharp increase in the intensity takes place over a narrow concentration range of the ligand (at about 1×10^{-5} mol L^{-1}) reaching a plateau with no further increase in the presence of excess ligand. This general feature has been observed with numerous types of DNA condensing agents (see Introduction), including small cationic peptides such as tetra- and penta- lysines [26,37]. We have previously reported on the ionic strength dependence of this effect [12], which is consistent with the electrostatic nature of the DNA binding [38] of oligolysines [39] and oligoarginines [40].

The intercalating dye ethidium is frequently used as a probe for DNA. Its fluorescence increases substantially when it is bound to DNA, and the decrease in this signal observed in the presence of DNA condensing agents has been attributed to displacement of the dye from condensed DNA [5,41–44]. The effect of penta-arginine in this

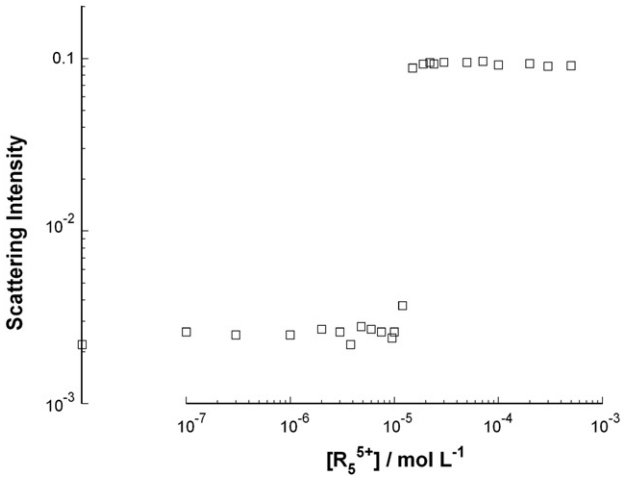

Fig. 2. Effect of penta-arginine (R_5^{5+}) concentration on light scattering by pUC18 plasmid DNA. The penta-arginine concentration at the *Y*-axis is zero. The composition of the solutions was identical to that described in Fig. 1. The intensity of light (wavelength λ = 350 nm, bandwidth Δλ = 5 nm) scattered at 90° was assayed with a fluorescence spectrometer by having both excitation and emission monochromators set to this wavelength.

assay is shown in Fig. 3. A modest decrease in fluorescence is observed at ligand concentrations of 5×10^{-6} to 8×10^{-6} mol L^{-1}, with a much sharper decrease (to 40–50%) at about 1×10^{-5} mol L^{-1}. An increase in fluorescence polarization from 0.12 to 0.14 can also be observed over this range of ligand concentration, indicating decreased motion of the bound ethidium within the condensate [44]. Higher concentrations of the ligand exhibit little further decrease in fluorescence intensity.

Circular dichroism was used to examine conformational response of the plasmid to binding of the penta-arginine ligand (Fig. 4). In these experiments, the plasmid concentration is held constant and the ligand concentration examined in the range of 1×10^{-6} mol L^{-1} to 3×10^{-5} mol L^{-1} (where Figs. 1–3 show effects on sedimentation, light scattering, and ethidium fluorescence). In the absence of any added ligand, the CD spectrum is typical of B-DNA with a positive band at around 280 nm. Concentrations of the ligand that are too low to produce condensation (as estimated by sedimentation and static light scattering) decrease the intensity of this signal but do not affect its peak position. After condensation of the plasmid at a ligand concentration of 1×10^{-5} mol L^{-1}, the intensity of the signal decreased further and its location shifted to a higher wavelength of 295 nm. These observations are consistent with previous reports obtained with other DNA condensing agents [6,43]. The decrease in the magnitude of the CD signal implies smaller base stacking interactions [5].

The hydrodynamic radius of the plasmid condensates was estimated by means of dynamic light scattering [34]. As in the CD observations described above, both uncondensed and condensed plasmids were examined. The results are summarized in Table 1. Both static and dynamic light scattering treatments assume spherical particles and this may not be valid for particles in the micron size range. Furthermore, the uncondensed and condensed plasmid is presumably randomly coiled and thus the hydrodynamic radius estimated by dynamic light scattering differs from the radius of gyration estimated by static light scattering [53]. The observed size includes other molecules that comigrate with the particle. Even though the values listed in Table 1 are semi-quantitative because of the systematic underestimation of particle sizes, the trend is consistent with plasmid condensation above the penta-arginine threshold concentration of 1×10–5 mol L^{-1}. The uncondensed

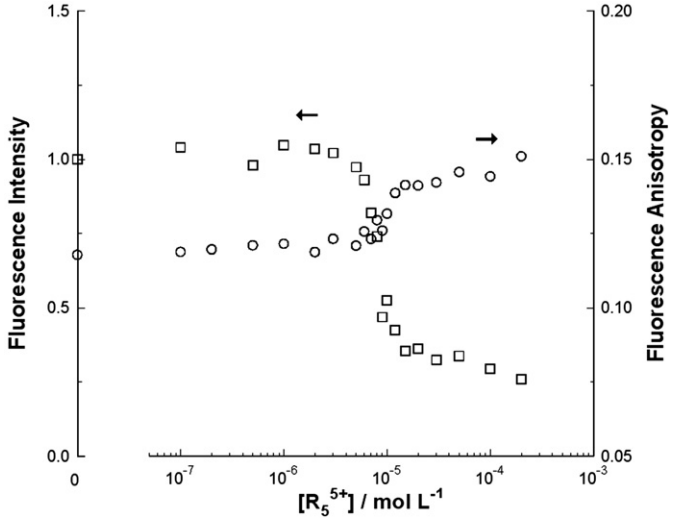

Fig. 3. Effect of penta-arginine (R_5^{5+}) concentration on the fluorescence intensity and the fluorescence polarization of plasmid bound ethidium. The composition of the solutions was identical to that described for Fig. 1, except for the additional presence of 1×10^{-6} mol L^{-1} ethidium. Both the fluorescence intensity (square, left *Y*-axis) and polarization (circle, right *Y*-axis) was monitored at an emission wavelength $\lambda_{em}=590$ nm with an excitation wavelength $\lambda_{ex}=510$ nm. The excitation and emission bandwidths were $\Delta\lambda=5$ and 10 nm respectively. The intensity was normalized to that in the absence of the ligand.

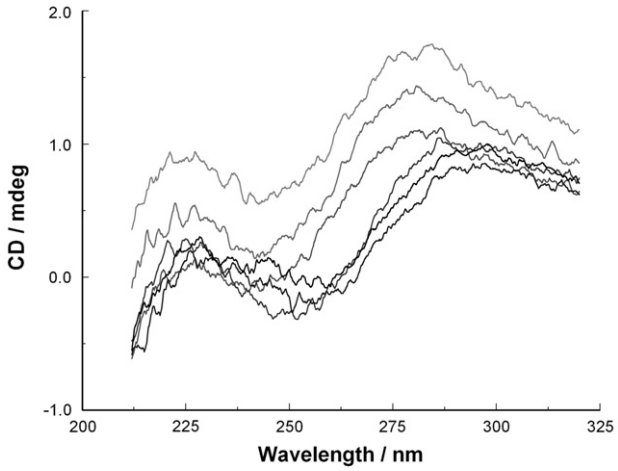

Fig. 4. Circular dichroism spectra of pUC18 in the presence of penta-arginine (zero, 1×10^{-6}, 5×10^{-6}, 10×10^{-6}, 20×10^{-6}, and 30×10^{-6} mol L^{-1}). Higher concentrations of the ligand are indicated by darker lines. Again the composition of the solution was otherwise identical to that described for Fig. 1.

plasmid is found to have a radius in the range of 70 to 80 nm. This agrees with previous reports [37,43] and is consistent with the expected rod-like intertwined double helices of length ca. 500 nm and diameter ca. 3–4 nm. Bimodal distributions were observed when the plasmid was condensed using penta-arginine. In the presence of excess ligand the radius of the major component was in the range of 4 μm, about 50-fold greater than that of the monomeric plasmid.

In DNA condensation, the interpretation of dynamic light scattering data can be complicated by the two effects of compaction and aggregation. Compaction of a single DNA macromolecule leads to a decrease in its size, while aggregation of multiple macromolecules has the opposite effect. The data in Table 1 for the condensation of plasmid pUC18 by penta-arginine provide an example of this, where the hydrodynamic radius shows a slight dependence on the ligand concentration. At a concentration just sufficient to produce condensation (1×10^{-5} mol L^{-1}), penta-arginine produces particles mostly in the 500 to 600 nm range. An increase in the ligand concentration of 2-fold to 2×10^{-5} mol L^{-1} increases the particle size by 7- to 8-fold. These observations suggest that extensive aggregation takes place after compaction is completed.

The presence of free plasmid DNA in the condensates was examined using atomic force microscopy in the tapping mode on dried samples. Typical images are reproduced in Fig. 5. Filamentous objects having both size and shape expected of individual plasmids (rods ca. 500 nm in length) are easily detectable in large numbers at a concentration of penta-arginine (5×10^{-6} mol L^{-1}) too low to produce condensation (Fig. 5A). They are not visible when the ligand

Table 1
Hydrodynamic radius data for plasmid pUC18 as a function of the penta-arginine (R_5^{5+}) concentration, as estimated by using dynamic light scattering. The experimental conditions are identical to those described for Figs. 1–4.

$[R_5^{5+}]$ /mol L^{-1}	Weighting	Radius *R*/nm		
		Mean	Standard deviation	Contribution (%)
5.0×10^{-6}	Intensity	79.3	17	100
	Volume	68.9	16	100
10×10^{-6}	Intensity	95.6	19	3
	Intensity	540	120	97
	Volume	85.6	17	19
	Volume	560	106	81
20×10^{-6}	Intensity	770	129	25
	Intensity	4020	910	75
	Volume	800	150	6
	Volume	4160	860	93

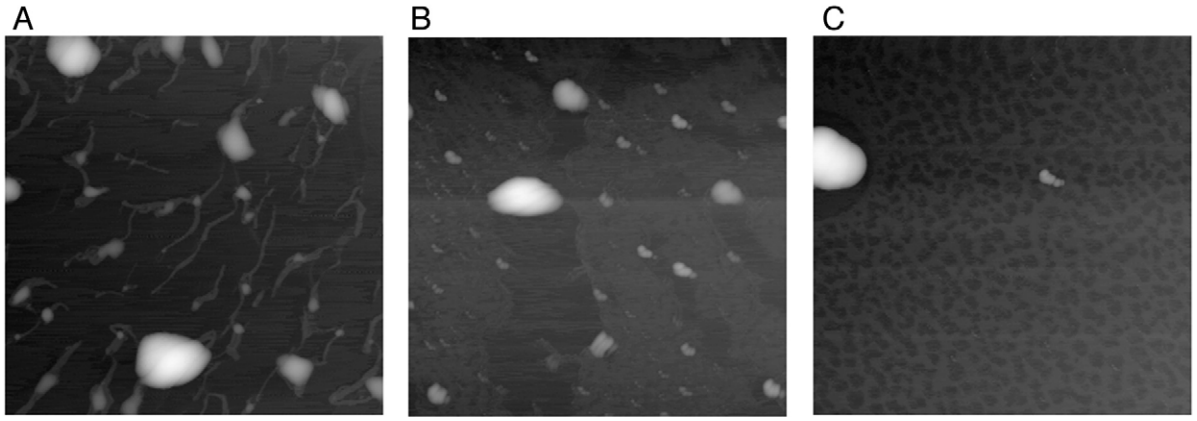

Fig. 5. Representative atomic force microscopy images of pUC18 in the presence of penta-arginine (A, 5×10^{-6}; B, 10×10^{-6}; and C, 20×10^{-6} mol L^{-1}) after air drying on mica. The images span 5 μm × 5 μm in the horizontal plane. Smaller distance in the vertical axis above this plane is indicated by darker pixels. The scale of the vertical axis is 4–5 nm. The composition of the solution was again otherwise identical to that described for Fig. 1.

concentration is increased by 2-fold to 1×10^{-5} mol L^{-1} (Fig. 5B) or 4-fold to 2×10^{-5} mol L^{-1} (Fig. 5C) to concentrations that bring about condensation of the plasmid (as estimated by sedimentation, light scattering, and ethidium fluorescence). There is no evidence for the toroidal structures frequently reported with DNA condensing ligands such as spermine [45]. Note that these samples are unirradiated and therefore no plasmid fragments are expected to be present [36].

Fig. 6 shows examples of typical radiosensitivity assays. Plasmid pUC18 was gamma irradiated under the same conditions used for Figs. 1 and 2. For clarity only three different concentrations of the penta-arginine ligand are shown. For each radiation dose, the fraction of the plasmid in the supercoiled form was quantified by using agarose gel electrophoresis. This fraction is plotted against the radiation dose. Increasing radiation produces a decrease in the fraction of supercoiled plasmid and a corresponding increase in the relaxed open circle or nicked conformation (not shown). This observation represents the introduction into the plasmid of single stand breaks (SSB). From the slope of a fitted straight line it is possible to derive the radiation chemical yield (by convention called a *G*-value) of these SSB products. This yield is represented by the symbol *G*(SSB) and has the unit mol J^{-1}. Values of *G*(SSB) calculated in this manner are plotted in Fig. 7 against the concentrations of one of three additives. These three additives are: (1) the ligand penta-arginine; (2) the well known and frequently studied DNA condensing agent hexa-ammine cobalt (III); and (3) the commonly used hydroxyl radical scavenger glycerol. The first two of these reagents produce a very sharp decrease in the SSB yield of about 100-fold over a very narrow concentration range of less than 2-fold at well defined concentrations of 1×10^{-5} mol L^{-1} (penta-arginine) and 1.5×10^{-4} mol L^{-1} (hexa-ammine cobalt(III)). In contrast achieving a decrease of a similar size in the SSB yield requires an increase in the glycerol concentration of several hundred times to the much larger concentration of about 10^{-1} mol L^{-1}.

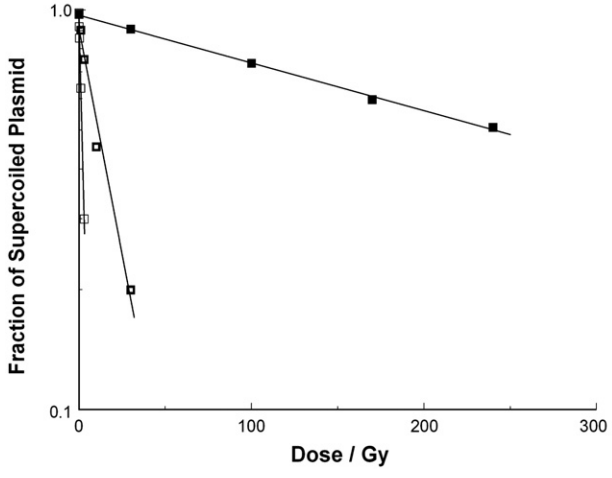

Fig. 6. Loss of supercoiled pUC18 with radiation dose. Aliquots of the solutions used to collect the data plotted in Fig. 1 were gamma irradiated in the dose range zero to 240 Gy. Examples are plotted here in Fig. 4 for penta-arginine concentrations of 5.0×10^{-6} (light open square), 7.1×10^{-6} (heavy open square), and 1.7×10^{-5} (closed square) mol L^{-1}. The fraction of supercoiled plasmid present after each dose was quantified by gel electrophoresis. The data sets are fitted with least mean square straight lines of the form $y=ce^{-mx}$. From the slopes *m*, the D_0 doses and SSB yields under the three conditions shown here are (light open square) 2.56 Gy, 2.23×10^{-3} μmol J^{-1}; (heavy open square) 19.2 Gy, 2.98×10^{-4} μmol J^{-1}; and (closed square) 364 Gy, 1.58×10^{-5} μmol J^{-1}.

4. Discussion

We present here a description of the physical and chemical properties of the complexes formed upon binding of the cationic ligand penta-arginine to the plasmid pUC18. The changes in physical properties such as sedimentation and light scattering are characteristic of an increase in particle size. Alterations of spectroscopic properties such as ethidium fluorescence and circular dichroism reflect changes in the DNA conformation. They are all typical of the behavior of well

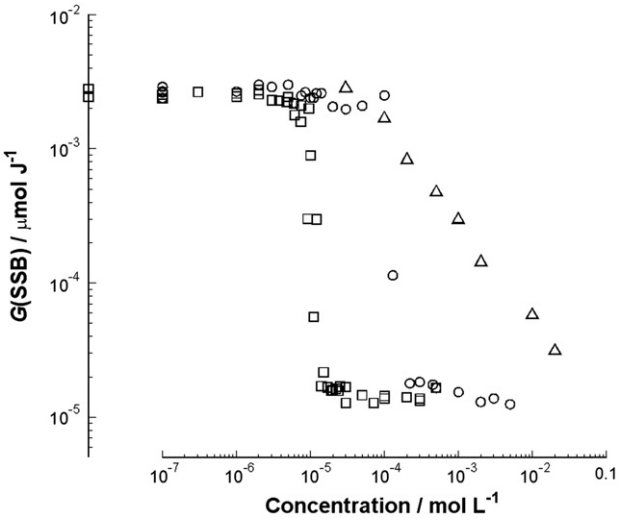

Fig. 7. Effect of penta-arginine (R_5^{5+}, square); hexa-ammine cobalt(III) (circle); or glycerol (triangle) concentrations on the SSB yield in gamma irradiated plasmid pUC18. The ligand concentration at the *Y*-axis is zero, although 1×10^{-5} mol L^{-1} glycerol was present. The SSB yield was quantified using the method shown in Fig. 4. Apart from glycerol and the ligand, the composition of the solutions was identical to that described for Fig. 1.

known and extensively studied DNA condensing agents such as hexa-ammine cobalt(III) [2] and the polyamines spermidine and spermine [3]. Large changes in behavior and structure are associated with condensation of the plasmid when the ligand concentration exceeds a sharply defined critical value. The general similarity between the cationic structure of penta-arginine and the other well known ligands and between the effect they all have on the physical properties of DNA strongly suggest that penta-arginine is able to behave as a DNA condensing agent. Using dynamic light scattering, it is possible to conclude that the sizes of the particles formed lies in the range of a few micrometers (Table 1). This is typically larger than the values of a few hundred nanometers observed with other more compact ligands [46]. It is possible that the branched structure of the oligopeptide may be responsible.

Recently it has become clear that in the case of radiobiology, the issue of DNA compaction is essential to understanding the relative contributions of the direct effect (damage produced by ionization of the DNA itself) and the indirect effect (damage produced by the reaction of reactive intermediates derived from water). There are several reports of a large attenuation of radiation induced DNA damage associated with condensation [12,26,47]. An example is shown in Fig. 7 under the same conditions used to examine the sedimentation, light scattering, and spectroscopic effects shown in Figs. 1–3 and in Table 1. A sharp decrease in the yield of DNA single strand breaks (SSB) is observed over a narrow concentration range of the penta-arginine ligand. This effect is also observed with hexa-ammine cobalt(III). Glycerol behaves in a fundamentally different manner and produces only a gradual change in the SSB yield.

In the radiolysis system we use here, SSB products in the plasmid are produced by its reaction with the hydroxyl radical ($^{\bullet}$OH) [20]. The hydroxyl radical is derived from the ionization of water, and so this is an example of the indirect effect of irradiation. The protective effect of glycerol (in concentrations in the millimolar to molar range) on the plasmid is due to its ability to competitively intercept •OH before they encounter the plasmid. Numerous other additives (also called scavengers) behave in this fashion having an efficiency which is proportional to their reactivity with $^{\bullet}$OH [48].

Hexa-ammine cobalt(III) also protects the plasmid against $^{\bullet}$OH attack, but the mechanism appears to be quite different. There is no evidence that the radioprotective effect of hexa-ammine cobalt(III) is directly related to its DNA binding, since the SSB yield is unaffected by it up to a concentration of about 1×10^{-4} mol L^{-1}. Condensation of DNA by hexa-ammine cobalt(III) and other oligo-cations typically requires neutralization of 89% to 90% of the negatively charged phosphates [3,37]. Therefore under conditions just insufficient to produce condensation, the plasmid must be extensively bound by the metal ligand. The SSB yield is dominated by the competition for $^{\bullet}$OH between the plasmid and the glycerol present in solution at 1×10^{-4} mol L^{-1}, since glycerol is at least 20-fold more reactive than hexa-ammine cobalt(III) with $^{\bullet}$OH [48]. However once condensation has taken place, the SSB yield decreases by about 100-fold (Fig. 7). A physical protection of the plasmid from the bulk of the solvent would appear to be the mechanism responsible for this very large effect since the nature of the condensing agent is unimportant. A very similar protective effect was observed for penta-arginine (Fig. 7) and for other cationic ligands [26]. We have reported previously on their ionic strength dependence, which is consistent with the electrostatic binding of the cationic oligo-arginine and oligo-lysine peptide ligands to the polyanionic plasmid DNA [12].

A large body of work on the radiation chemistry and the radical chemistry of DNA and of its component functional groups suggests that reactions with water and with dissolved oxygen are very important [19,25] in the formation of the stable end products observed in vitro and in vivo [49]. It is possible that these reactions may not be well modeled by experimental systems that attenuate the indirect effect by dehydration and/or with cryogenic temperatures [21,22,50–52]. We argue that they are more likely to be faithfully reproduced by DNA condensed with a cationic ligand in dilute aqueous solution.

We described in the Introduction that condensed DNA may be exploited as a model system with which to examine DNA damage by the direct effect of ionizing radiation (ionization of the DNA itself). This process is very inefficient in dilute aqueous solution because most ionization events take place in the vast excess of water and the major route to DNA damage is from reactive intermediates derived from water (the indirect effect), mainly the hydroxyl radical. Condensed DNA is however extensively protected from the bulk of the solvent and it is significantly less accessible to freely diffusible solutes. The physical data reported here provides a more thorough characterization of this model system.

Acknowledgements

Supported by PHS grant CA46295. The authors wish to thank Dr. Jonathan Neidigh (Department of Biochemistry, Loma Linda University) for the assistance with CD spectroscopy.

References

[1] V.A. Bloomfield, DNA condensation, Curr. Opin. Struct. Biol. 6 (1996) 334–341.
[2] J. Widom, R.L. Baldwin, Cation induced toroidal condensation of DNA: studies with $Co^{3+}(NH_3)_6$, J. Mol. Biol. 144 (1980) 431–453.
[3] V. Vijayanathan, T. Thomas, A. Shirahata, T.J. Thomas, DNA condensation by polyamines: a laser light scattering study of structural effects, Biochemistry 40 (2001) 13644–13651.
[4] M. Keller, T. Tagawa, M. Preuss, A.D. Miller, Biophysical characterization of the DNA binding and condensing properties of adenoviral peptide *mu*, Biochemistry 41 (2002) 652–659.
[5] A.M. del Pozo, V. Lacadena, J.M. Mancheno, N. Olmo, M. Onaderra, J.G. Gavilanes, The antifungal protein AFP of *Aspergillus giganteus* is an oligonucleotide/oligosaccharide binding (OB) fold containing protein that produces condensation of DNA, J. Biol. Chem. 277 (2002) 46179–46183.
[6] M. Rosa, N. Penacho, S. Simoes, M.C.P. Lima, B. Lindman, M.G. Miguel, DNA pre-condensation with an amino acid based cationic amphiphile. A viable approach for liposome based gene delivery, Mol. Membrane Biol. 25 (2008) 23–34.
[7] J.E. Ramos Jr, J.R. Neto, R. de Vries, Polymer induced condensation of DNA supercoils, J. Chem. Phys. 129 (2008) 185102.
[8] N.V. Hud, K.H. Downing, R. Balhorn, A constant radius of curvature model for the organization of DNA in toroidal condensates, Proc. Natl. Acad. Sci. U. S. A. 92 (1995) 3581–3585.
[9] I.D. Vilfan, C.C. Conwell, T. Sarkar, N.V. Hud, Time study of DNA condensate morphology: implications regarding the nucleation, growth, and equilibrium populations of toroids and rods, Biochemistry 45 (2006) 8174–8183.
[10] P.G. Arscott, A.Z. Li, V.A. Bloomfield, Condensation of DNA by trivalent cations. 1. Effects of DNA length and topology on the size and shape of condensed particles, Biopolymers 30 (1990) 619–630.
[11] J.-R. Daban, High concentration of DNA in condensed chromatin, Biochem. Cell Biol. 81 (2003) 91–99.
[12] A. Ly, S. Bullick, J.H. Won, J.R. Milligan, Cationic peptides containing tyrosine protect against radiation-induced oxidative DNA damage, Int. J. Radiat. Biol. 82 (2006) 421–433.
[13] W. Wang, D. Becker, M.D. Sevilla, The influence of hydration on the absolute yields of primary ionic free radicals in gamma-irradiated DNA at 77 K. I. Total radical yields, Radiat. Res. 135 (1993) 146–154.
[14] L.I. Shukla, R. Pazdro, D. Becker, M.D. Sugar, Sugar radicals in DNA: isolation of neutral radicals in gamma-irradiated DNA by hole and electron scavenging, Radiat. Res. 163 (2005) 591–602.
[15] J.D. Chapman, A.P. Reuvers, J. Borsa, C.L. Greenstock, Chemical radioprotection and radiosensitization of mammalian cells growing in vitro, Radiat. Res. 56 (1973) 291–306.
[16] C.F. Webb, G.D. Jones, J.F. Ward, D.J. Moyer, J.A. Aguilera, L.L. Ling, Mechanisms of radiosensitization in bromodeoxyuridine substituted cells, Int. J. Radiat. Biol. 64 (1993) 695–705.
[17] J.A. LaVerne, I. Stefanic, S.M. Pimblott, Hydrated electron yields in the heavy ion radiolysis of water, J. Phys. Chem. A 109 (2005) 9393–9401.
[18] J.W.T. Spinks, R.J. Woods, An introduction to radiation chemistry, 3rd edition Wiley, New York, 1990.
[19] C. von Sonntag, The chemical basis of radiation biology, Taylor and Francis, Philadelphia, 1987.
[20] J.R. Milligan, J.A. Aguilera, J.F. Ward, Variation of single-strand break yield with scavenger concentration for plasmid DNA irradiated in aqueous solution, Radiat. Res. 133 (1993) 151–157.
[21] K.K. Sharma, J.R. Milligan, W.A. Bernhard, Multiplicity of DNA single-strand breaks produced in pUC18 exposed to the direct effects of ionizing radiation, Radiat. Res. 170 (2008) 156–162.

[22] S.G. Swarts, D. Becker, M. Sevilla, K.T. Wheeler, Radiation induced DNA damage as a function of hydration. II. Base damage from electron loss centers, Radiat. Res. 145 (1996) 304–314.
[23] J.R. Milligan, J.F. Ward, Yield of single-strand breaks due to attack on DNA by scavenger-derived radicals, Radiat. Res. 137 (1994) 295–299.
[24] J.R. Milligan, J.Y.-Y. Ng, C.C. Wu, J.A. Aguilera, J.F. Ward, Y.W. Kow, S.S. Wallace, R.P. Cunningham, Methylperoxyl radicals as intermediates in the damage to DNA irradiated in aqueous dimethyl sulfoxide with gamma rays, Radiat. Res. 146 (1996) 436–443.
[25] C. von Sonntag, Free radical induced DNA damage and its repair. A chemical perspective, Springer, New York, 2006.
[26] G.L. Newton, A. Ly, N.Q. Tran, J.F. Ward, J.R. Milligan, Radioprotection of plasmid DNA by oligolysines, Int. J. Radiat. Biol. 80 (2004) 643–651.
[27] S. He, P.G. Arscott, V.A. Bloomfield, Condensation of DNA by multivalent cations: experimental studies of condensation kinetics, Biopolymers 53 (2000) 329–341.
[28] K.E. van Holde, Chromatin, Springer, New York, 1988.
[29] M. Spotheim-Maurizot, S. Ruiz, R. Sabattier, M. Charlier, Radioprotection of DNA by polyamines, Int. J. Radiat. Biol. 68 (1995) 571–577.
[30] S. Chiu, N.L. Oleinick, Radioprotection of cellular chromatin by the polyamines spermine and putrescine: preferential action against formation of DNA-protein crosslinks, Radiat. Res. 149 (1998) 543–549.
[31] R.L. Warters, G.L. Newton, P.L. Olive, R.C. Fahey, Radioprotection of human cell nuclear DNA by polyamines. Radiosensitivity of chromatin is influenced by tightly bound spermine, Radiat. Res. 151 (1999) 354–362.
[32] J.R. Milligan, N.Q. Tran, A. Ly, J.F. Ward, Peptide repair of oxidative DNA damage, Biochemistry 43 (2004) 5102–5108.
[33] C. Houee-Levin, C. Sicard-Roselli, Radiation chemistry of proteins, in: C. Jonah, B. Rao (Eds.), Radiation chemistry, present status and future prospects, Elsevier, New York, 2001, pp. 553–584.
[34] V.A. Bloomfield, Quasi-elastic light scattering applications in biochemistry and biology, Ann. Rev. Biophys. Bioeng. 10 (1981) 421–450.
[35] D. Pang, J.E. Rodgers, B.L. Berman, S. Chasovskikh, A. Dritschilo, Spatial distribution of radiation induced double strand breaks in plasmid DNA as resolved by atomic force microscopy, Radiat. Res. 164 (2005) 755–765.
[36] K. Psonka, E. Gudowska-Nowak, S. Brons, T. Elsasser, M. Heiss, G. Taucher-Scholz, Ionizing radiation induced fragmentation of plasmid DNA. Atomic force microscopy and biophysical modeling, Adv. Space Res. 39 (2007) 1043–1049.
[37] I. Nayvelt, T. Thomas, T.J. Thomas, Mechanistic differences in DNA nanoparticle formation in the presence of oligolysines and poly-L-lysine, Biomacromolecules 8 (2007) 477–484.
[38] S. Padmanabhan, W. Zhang, M.W. Capp, C.F. Anderson, M.T. Record Jr, Binding of cationic (+4) alanine and glycine containing oligopeptides to double stranded DNA: thermodynamic analysis of effects of coulombic interactions and α-helix induction, Biochemistry 36 (1997) 5193–5206.
[39] D.P. Mascotti, T.M. Lohman, Thermodynamic extent of counterion release upon binding oligolysines to single stranded nucleic acids, Proc. Natl. Acad. Sci. U. S. A. 87 (1990) 3142–3146.
[40] D.P. Mascotti, T.M. Lohman, Thermodynamics of oligoarginines binding to RNA and DNA, Biochemistry 36 (1997) 7272–7279.
[41] O.A.A. Ahmed, N. Adjimatera, C. Pourzand, I.S. Blagbrough, N4, N9-Dioleoyl spermine is a novel nonviral lipopolyamine vector for plasmid DNA formulation, Pharmaceut. Res. 22 (2005) 972–980.
[42] M. Wittmar, J.S. Ellis, F. Morell, F. Unger, J.C. Schumacher, C.J. Roberts, S.J.B. Tendler, M.C. Davies, T. Kissel, Biophysical and transfection studies of an amine modified poly(vinyl alcohol) for gene delivery, Bioconjug. Chem. 16 (2005) 1390–1398.
[43] L.E. Prevette, T.E. Kodger, T.M. Reineke, M.L. Lynch, Deciphering the role of hydrogen bonding in enhancing pDNA-polycation interactions, Langmuir 23 (2007) 9773–9784.
[44] A.M.L. Ny, C.T. Lee Jr., Conformation and dynamics of DNA molecules during photoreversible condensation, Biophys. Chem. 142 (2009) 76–83.
[45] V. Vijayanathan, T. Thomas, T. Antony, A. Shirahata, T.J. Thomas, Formation of DNA nanoparticles in the presence of novel polyamine analogues: a laser light scattering and atomic force microscopic study, Nucleic Acids Res. 32 (2004) 127–134.
[46] C.C. Conwell, I.D. Vilfan, N.V. Hud, Controlling the size of nanoscale toroidal DNA condensates with static curvature and ionic strength, Proc. Natl. Acad. Sci. U. S. A. 100 (2003) 9296–9301.
[47] G.L. Newton, J.A. Aguilera, J.F. Ward, R.C. Fahey, Polyamine-induced compaction and aggregation of DNA: a major factor in radioprotection of chromatin under physiological conditions, Radiat. Res. 145 (1996) 776–780.
[48] G.V. Buxton, C.L. Greenstock, W.P. Helman, A.B. Ross, Critical review of rate constants for reactions of hydrated electrons, hydrogen atoms, and hydroxyl radicals in aqueous solution, J. Phys. Chem. Ref. Data 17 (1988) 513–887.
[49] J. Cadet, T. Douki, J.-L. Ravanat, Oxidatively generated damage to the guanine moiety of DNA. Mechanistic aspects and formation in cells, Acc. Chem. Res. 41 (2008) 1075–1083.
[50] C. Pal, J. Huettermann, Postirradiation electron transfer vs differential radical decay in X-irradiated DNA and its mixtures with additives. Electron spin resonance spectroscopy in LiBr glass at low temperatures, J. Phys. Chem. B 110 (2006) 14976–14987.
[51] A. Adhikary, D. Khanduri, M.D. Sevilla, Direct observation of the hole protonation state and hole localization site in DNA-oligomers, J. Am. Chem. Soc. 131 (2009) 8614–8619.
[52] A. Yokoya, S.M. Cunniffe, R. Watanabe, K. Kobayashi, P. O'Neill, Induction of DNA strand breaks, base lesions, and clustered damage sites in hydrated plasmid DNA films by ultrasoft X-rays around the phosphorus K edge, Radiat. Res. 172 (2009) 296–305.
[53] V. Trappe, J. Bauer, M. Weissmueller, W. Burchard, Angular dependence in static and dynamic light scattering from randomly branched systems, Macromolecules 30 (1997) 2365–2372.